

Classical dynamics of triatomic systems: Energized harmonic molecules*

C. A. Parr[†] and A. Kuppermann

Arthur A. Noyes Laboratory of Chemical Physics,[†] California Institute of Technology, Pasadena, California 91125

R. N. Porter

Department of Chemistry, State University of New York, Stony Brook, Long Island, New York 11790

(Received 26 March 1976)

The dynamical assumptions underlying the Slater and RRK classical-mechanical theories of unimolecular reaction rates are investigated. The predictions of these theories for several nonlinear, triatomic, harmonically bonded molecular models are compared with the results obtained from the integration of the classical equations of motion. The accuracy of the small-vibration and weak-coupling assumptions are found to break down at energies above about one-quarter of a bond dissociation energy. Nonetheless, the small-vibration approximation predicts reaction frequencies in good agreement with the exact results for the models. The effects of rotation on intramolecular energy exchange are examined and found to be significant.

I. INTRODUCTION

Some widely applied theories of the rates of thermal unimolecular decomposition and isomerization of polyatomic molecules¹⁻⁶ rest upon the assumption of noninteracting harmonic vibrations for their tractability. In either a classical or quantum-mechanical formulation, this assumption leads to the familiar⁷ separation of the total nuclear Hamiltonian into a sum of mutually commuting normal-mode, harmonic-oscillator Hamiltonians whose eigenvalues, the normal-mode energies, are constants of the motion. In practice, the normal-mode frequencies required for an *a priori* dynamical attack on the problem of unimolecular processes of energized molecules are obtained directly from spectroscopic observation or by extrapolation from spectroscopic results for similar molecules. Since these data can be expected to describe the potential-energy surface best in the immediate vicinity of the minimum, it is appropriate to ask to what extent such a harmonic normal-mode treatment can describe the dynamics of a real, energized molecule at the substantially higher energies usually required for it to undergo dissociation or isomerization.

Several simple potential-energy expressions have been used to fit spectroscopic data.⁸ In this paper we employ the simplest of these expressions, namely, the "central force field" (hereinafter designated CFF) for its relative ease of calculation. The harmonic CFF model for the potential energy is a diagonalized quadratic form in the interatomic distances for each pair of atoms, whether these are "bonded" or "nonbonded" in the usual valence sense. Although harmonic in the bond stretches, in the case of nonlinear molecules the harmonic CFF model leads to interaction terms when the energy is expanded in the normal-mode displacements. Thus, an important result is that in both the classical and quantum-mechanical harmonic treatments of molecular vibration, the normal-mode energies are constants of the motion *only* in the limit of infinitesimal displacements of the atoms from their equilibrium geometry. Since in one version of the Slater unimolecular rate theory⁹ it is assumed that the normal-mode energies are

rigorous constants of the motion even when vibration amplitudes approach values characteristic of the reaction threshold, in Secs. VII. A.1–VII. A.4 we assess the effects of deviation from the small-vibration approximation (SVA) which are included in the harmonic CFF model. In the Slater treatment,⁹ reaction occurs when some critical coordinate (or coordinates)¹⁰ is stretched or compressed to a critical value. The reaction rate depends in part upon the frequency with which the critical coordinate attains its critical value. In Sec. VII. A.5, we determine the sensitivity of this reaction frequency to the breakdown of the SVA. In Sec. VII. B we investigate the perturbing effect of rotation.

The Rice–Ramsberger–Kassel (RRK) theory² of unimolecular decomposition considers molecules to be sets of harmonic oscillators coupled together strongly enough to allow energy to flow freely between them but weakly enough that the total vibration energy is given by the sum of the oscillator energies.¹¹

Recently, experimental evidence has been accumulating which challenges the validity of these assumptions. It includes the results of vibronic level fluorescence,¹² crossed molecular beams,¹³ mass spectrometry,¹⁴ and infrared laser augmented decompositions.¹⁵ In the present paper we make a direct test of the dynamical assumptions just mentioned against classical trajectory calculations of harmonic CFF model molecules. The oscillators which form the basis for the original Kassel theory were defined merely as "harmonic degrees of freedom."¹⁶ The term "oscillator" could conceivably apply to the interatomic bonds or to the normal modes; each of these interpretations is examined here.

Marcus' extension⁶ of RRK theory is a purely phase-space theory dealing with statistical ensembles of energized molecular systems. It may be applied to reacting system where either the energizing process or the subsequent unimolecular dynamics (preferably both) populate the molecular states statistically. Furthermore, the statistical distribution of states must be maintained even under the perturbation of depopulation by reaction. Thus a sufficient condition for the maintenance of a

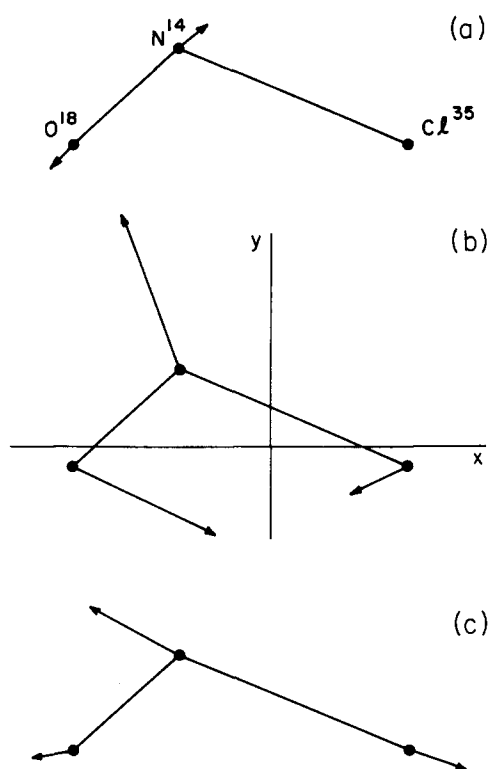


FIG. 1. Equilibrium configuration and normal modes of ClN^{18}O : (a) asymmetric stretch, (b) bend, (c) symmetric stretch. Arrows represent exaggerated atomic displacements corresponding to a normal-mode energy equal to 8 times the N-Cl dissociation energy. The lack of an arrow in (a) associated with the Cl atom indicates the smallness of its displacement in this mode.

statistical distribution is the RRK assumption of free flow of energy among the molecule's oscillators. (This would become a necessary condition, if the energizing process biased the resultant initial molecular states.) This intramolecular energy flow should be more rapid than any reactive event in order to avoid non-RRKM behavior. The significance of this free flow will be examined in Sec. VII.

We limit ourselves to the simplest system of interest in unimolecular decomposition studies, namely, the triatomic molecule. Although the equations of motion of general three-body systems cannot be solved analytically in either classical or quantum-mechanical formulations, they yield readily to numerical solution in the classical case, and progress has been made in the solution of the quantum problem.¹⁷ It should be noted that an accurate quantum-mechanical solution is not

necessary for the verification of the conservation of dynamical variables. For conservative systems, the correspondence principle insures that a dynamical variable is a quantum-mechanical constant of the motion if, and only if, it is a classical constant of the motion as well.¹⁸ Thus, the classical atomic trajectory calculations we report here suffice to test the constancy of normal-mode energies assumed in Slater's theory and the constancy of the sum of the energies assumed in the weak-coupling theories, even though interference might lead to quantum effects in other dynamical attributes.

We analyze the zero-point-energy dynamics (Sec. VII. A.1) of CFF models of several nonlinear molecules (H_2O , D_2S , H_2Se , NO_2 , SO_2 , and F_2O and ClN^{18}O) as well as the high-energy dynamics (Sec. VII. A.2-VII. A.4) of two such models to test the assumptions of the theories mentioned above. The first high-energy model molecule, designated A_3 , is a somewhat artificial one consisting of three point particles of equal mass connected pairwise by three identical harmonic "bonds." In their equilibrium geometry, the mass points are thus located at the vertices of an equilateral triangle. (This D_{3h} symmetry forces the degeneracy of A_3 's bends and asymmetric stretch vibration modes.) The use of a dimensionless form for the equations of motion enables one to interpret the results in terms of an infinite number of sets of model parameters. For simplicity, we shall discuss A_3 in terms of only one such set, wherein the masses all correspond to ^{16}O , the bond force constants and equilibrium lengths all correspond to the O_2 molecule,¹⁹ and the dissociation energy, $2D_0$, is taken to be twice that of molecular oxygen. The second high-energy harmonic CFF model is a more realistic one for nitrosyl chloride, ClN^{18}O , wherein the experimental molecular structure²⁰ (see Fig. 1), harmonic CFF force constants,²¹ and dissociation energy²² are used. The model and molecular parameters of the molecules investigated in greater detail are given in Table I.

II. PREVIOUS CLASSICAL UNIMOLECULAR TRAJECTORY STUDIES

Thiele and Wilson²³ used classical-mechanical trajectory calculations to indicate the impropriety of the application of the SVA to in-line vibrations of linear *anharmonic* molecules. When chemically interesting energies were introduced into an anharmonic model for CO_2 , the rigorous solution of the equations of motion gave normal coordinates which were aperiodic functions of time. Normal-mode energies were not reported, but the failure of the SVA can be expected to have been re-

TABLE I. Model and molecular parameters.

Model ^a	(\AA)				(mdyn/ \AA)			(cm ⁻¹)		
	r_1^{eq}	r_2^{eq}	r_3^{eq}	θ_2^{eq} ^b	k_1	k_2	k_3	ω_{sym}	ω_{asym}	ω_{bend}
HOH	0.957	1.514	0.957	104.5°	8.45	1.78	8.45	4376	3934	1380
A_3	1.207	1.207	1.207	60°	11.77	11.77	11.77	1931	1370	1370
¹⁸ ONCl	1.975	2.650	1.139	114°	1.92	0.98	13.97	592	1750	329

^aSee Fig. 1 for definitions of bond labels.

^bAngle opposite bond 2.

flected by their nonconstancy.

In the first of his papers on the classical-mechanical calculation of triatomic dissociation rates, Bunker^{24a} investigated the kinetics of three classical harmonic molecular models, two for linear N_2O and one for bent O_3 . His results indicate that these models apparently have metrically decomposable²⁵ phase spaces associated with nonergodic behavior.¹⁷ The normal mode coordinates appear to be almost periodic functions of time, and many trajectories with energies in excess of that required for dissociation failed to react during the observation time (about 50 symmetric stretch periods). This nonergodicity persisted when rotation was included in the model.^{24b} For these models the Slater frequency factor²⁶ $\bar{\nu}$ agreed well with k_∞ , the high-pressure limit of the rate constant obtained from the Monte Carlo trajectory calculations. This implies that the Slater treatment accurately predicts the distribution of model lifetimes as they become arbitrarily short.

Hung and Wilson²⁷ investigated the classical dynamics of a rotating harmonic CFF model for CO_2 . Since the model was constrained to linearity, the nonrotating dynamics were strictly harmonic (see Sec. IV.B); that is, they followed the SVA predictions at all energies. Hung and Wilson found that rotation did *not* alter the harmonic vibrations significantly. Such behavior appears to validate the assumption implicit in the Slater and RRK theories that the dynamic efforts of vibration-rotation interaction may be ignored. However, as we shall see in Sec. VII, *nonlinear* harmonic CFF models do *not* follow SVA dynamics. The importance of the vibration-rotation interaction in the nonlinear models might thus be expected to be greater than that in the models constrained to linear vibrations. In the same paper, Hung and Wilson²⁷ found the effects of rotation on an anharmonic linear triatomic model were severe. Hung's extension of that investigation to four-atom linear models²⁸ confirm the sensitivity of anharmonic vibration dynamics to rotation.

Bunker and co-workers^{24c-e} have analyzed the thermal and hot-atom unimolecular isomerization and decomposition of 3-d anharmonic CH_3NC , concluding that the vibrationally-rotationally excited molecule is probably not RRKM.⁶ In other words, localized vibrational energy does not redistribute itself among all vibration modes rapidly compared with reaction rates. The energies used in those studies were well in excess of the isomerization ($\text{CH}_3\text{NC} \rightarrow \text{CH}_3\text{CN}$) threshold of 38 kcal mol⁻¹, and the time evolution of the model's normal-mode energies or coordinates were not reported. While Bunker indicates^{24c} that the hot-atom-induced isomerization is controlled more by rotation than vibration, still the failure of vibrational energies to circulate freely throughout this highly energized anharmonic model suggests that its reactions are nonergodic, at least on a reaction time scale. The observation^{24d} of RRKM-like decomposition ($\text{CH}_3\text{NC} \rightarrow \text{H} + \text{CH}_2\text{NC}$) implies that the vibration modes uncoupled from the isomerization coordinate may well be exchanging energy among themselves rapidly as required by the RRK² model.

III. CLASSICAL-MECHANICAL EQUATIONS OF MOTION

Let m_i and \mathbf{X}_i be the masses and position vectors of the nuclei of a triatomic molecule with respect to its center of mass. If \mathbf{X}_1 and \mathbf{X}_3 are taken to be the coordinates, the kinetic energy for the system is given by

$$T = \frac{1}{2} [(m_2 + m_3) \mathbf{P}_1 \cdot \mathbf{P}_1 / m_1 - \mathbf{P}_1 \cdot \mathbf{P}_3 + (m_1 + m_2) \mathbf{P}_3 \cdot \mathbf{P}_3 / m_3] (M)^{-1}, \quad (1)$$

where $M = \sum_{i=1}^3 m_i$, and \mathbf{P}_i are the momenta conjugate²⁹ to \mathbf{X}_i ($i=1, 3$). The potential energy function, in the harmonic model considered in this paper, is given by

$$V = \sum_{i=1}^3 V_i = \frac{1}{2} \sum_{i=1}^3 k_i (r_i - r_i^{\text{eq}})^2, \quad (2)$$

where k_i are the CFF constants, and r_i are the interatomic distances (see Fig. 2). The V_i are functions of the coordinates but not the momenta. The Hamilton equations of motion are

$$\begin{aligned} \dot{\mathbf{X}}_1 &= [(m_2 + m_3) \mathbf{P}_1 / m_1 - \mathbf{P}_3] (M)^{-1} \\ \dot{\mathbf{X}}_3 &= [(m_1 + m_2) \mathbf{P}_3 / m_3 - \mathbf{P}_1] (M)^{-1}, \end{aligned} \quad (3)$$

and

$$\dot{\mathbf{P}}_i = - \sum_{j=1}^3 (\partial V / \partial r_j) (\partial r_j / \partial \mathbf{X}_i) \quad (i=1, 3). \quad (4)$$

IV. SMALL VIBRATION APPROXIMATION

The small-vibration approximation (SVA) consists of the assumption that when the many-body equations of motion corresponding to Eqs. (3) and (4) are expanded in the atomic displacement coordinates, $\mathbf{X}_i - \mathbf{X}_i^{\text{eq}}$, terms of higher order than linear in these coordinates may be ignored. Under this assumption, the normal-mode coordinates are related to the atomic displacement ones by linear transformations which can be used to decouple the equations of motion. It can be shown³⁰ that in nonlinear molecules the SVA often leads to a violation of angular momentum conservation for nonvanishing vibra-

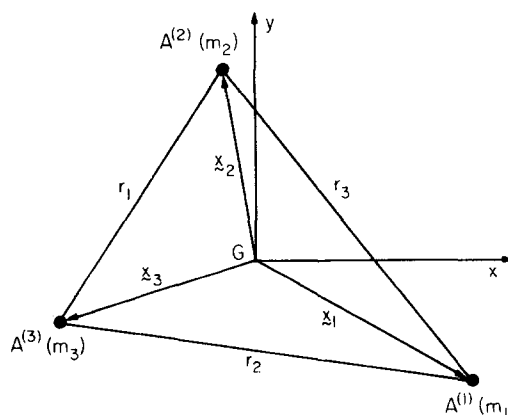


FIG. 2. Instantaneous configuration of the triatomic molecule $A^{(1)} A^{(2)} A^{(3)}$. G is the center of mass of the system, \mathbf{x}_i are the position vectors of the atoms $A^{(i)}$ with respect to G , m_i are their masses, and r_i the internuclear distances. Gx and Gy are Eckart system coordinate axis described in Sec. IV. A.

tion amplitudes. This violation persists even in nonrotating molecules, but it obviously becomes severe unless the equilibrium coordinates follow the molecule as it rotates. This is achieved by attaching to the triatomic system a body-fixed system of coordinates. Since this molecule is nonrigid, the choice of such a coordinate system is not unique. One such choice³¹ is to utilize the instantaneous principal axes of inertia of the molecule as coordinate axes. In this paper we will use the Eckart rotating coordinate system described below.³²

A. Eckart rotating coordinate system

The position vector of the i th atom in the nonrotating, center-of-mass system, is denoted by \mathbf{X}_i . The same vector in the rotating Eckart center-of-mass coordinate system (hereinafter referred to simply as the Eckart system) is denoted by \mathbf{x}_i . The Euler angles^{33a} ψ , θ , ϕ of the Eckart system with respect to the laboratory-fixed one, and the matrix \mathbf{U} which transforms the components of \mathbf{X}_i into those of \mathbf{x}_i via

$$\mathbf{x}_i = \mathbf{U} \mathbf{X}_i = \mathbf{U}_\psi \mathbf{U}_\theta \mathbf{U}_\phi \mathbf{X}_i, \quad (5)$$

are determined by the Eckart condition^{33b}

$$\sum_{i=1}^3 m_i (\mathbf{x}_i^{\text{eq}} \times \mathbf{x}_i) = 0. \quad (6)$$

The \mathbf{x}_i^{eq} in Eq. (6) are the vectors, fixed in the Eckart system, which locate the equilibrium positions of the nuclei. We require in addition that the vector $\hat{\mathbf{z}}$ be normal to the molecular plane. The angles θ and ϕ are then merely the spherical polar angles of the normal to the molecular plane in the laboratory-fixed system of reference. If we define an intermediate coordinate system in which

$$\mathbf{x}'_i = \mathbf{U}_\theta \mathbf{U}_\phi \mathbf{X}_i, \quad (7)$$

then from Eqs. (5)–(7) we obtain

$$\psi = \arctan(n/d), \quad (8)$$

where

$$n = \sum_{i=1}^3 m_i (x_i^{\text{eq}} Y'_i - y_i^{\text{eq}} X'_i) \quad (9)$$

and

$$d = \sum_{i=1}^3 m_i (x_i^{\text{eq}} X'_i + y_i^{\text{eq}} Y'_i). \quad (10)$$

The proper quadrant for ψ is chosen to maximize the quantity $\mathbf{x}_1 \cdot \mathbf{x}_1^{\text{eq}} + \mathbf{x}_2 \cdot \mathbf{x}_2^{\text{eq}}$, thereby insuring that the \mathbf{x}_i lie near and not opposed to the \mathbf{x}_i^{eq} .

B. Normal modes and energies

The details of the eigenvector–eigenvalue problem for the determination of molecular vibration frequencies and normal modes of motion are treated in Wilson, Decius, and Cross^{33c} and other standard texts. Intramolecular vibration potentials are given in terms of a set of internal coordinates, S_i . In the present case, the S_i are the three interatomic bond displacements, $r_i - r_i^{\text{eq}}$, and according to Eq. (2), V is a linear combination of the squares of these quantities. The relation between

the S_i and the \mathbf{x}_i is given by

$$S_i = [(x_j - x_k)^2 + (y_j - y_k)^2]^{1/2} - [(\bar{x}_j^{\text{eq}} - \bar{x}_k^{\text{eq}})^2 + (\bar{y}_j^{\text{eq}} - \bar{y}_k^{\text{eq}})^2]^{1/2} = r_i - r_i^{\text{eq}}, \quad (11)$$

where i, j, k is a cyclic permutation of 1, 2, 3. In the SVA, the linear transformation \mathbf{M} , obtained from Eq. (11), which relates the atomic displacements $x_i - x_i^{\text{eq}}$ to the S_i for infinitesimally small displacements from equilibrium geometry is assumed to be valid for all molecular geometries. Thus, if \mathbf{S} is a vector whose components are the S_i ($i=1, 2, 3$), and \mathbf{D} is a vector whose components are the atomic displacements $x_1 - x_1^{\text{eq}}$, $y_1 - y_1^{\text{eq}}$, and $x_3 - x_3^{\text{eq}}$, the relation

$$\mathbf{S} = \mathbf{M} \mathbf{D} \quad (12)$$

is assumed to hold in the SVA for large displacements as well as small ones. By the GF method,³³ a linear transformation \mathbf{L} may be found which relates the internal coordinates to the normal coordinates, Q_i , namely,

$$\mathbf{Q} = \mathbf{L}^{-1} \mathbf{S}, \quad (13)$$

where \mathbf{Q} is the vector of normal coordinates Q_i , in terms of which, in the SVA, V is still a linear combination of their squares and in addition T is a linear combination of the squares of their time-derivatives. Solution of the classical equations of motion for the Q_i gives

$$Q_i(t) = (2\epsilon_i/\lambda_i)^{1/2} \cos(\lambda_i^{1/2} t + \delta_i), \quad (14)$$

where ϵ_i and δ_i are the normal-mode energies and phase angles (both constants of the motion in the SVA), t is time, and the eigenvalues λ_i of the GF matrix are related to the molecular frequencies ν_i by

$$\lambda_i = 4\pi^2 \nu_i^2. \quad (15)$$

The normal-mode energies are related to the \dot{Q}_i and Q_i by

$$\epsilon_i = \frac{1}{2} \dot{Q}_i^2 + \frac{1}{2} \lambda_i Q_i^2, \quad (16)$$

and add up to a total normal energy ϵ which, in the SVA is constant and equal to the total vibration energy E . Interatomic bond distances in nonlinear molecules are quadratically related to the atomic displacements. The linear relation [Eq. (12)] between the bond displacements and the actual atomic displacements is in error at nonzero vibration amplitudes. This error causes the sum of the normal-mode energies ϵ to differ from the total vibration energy E in general. The difference between E and ϵ will be called the normal-mode energy defect.

C. Reactive excursion frequencies

The frequency with which some chosen coordinate in a harmonic molecule attains a critical value is called the reactive excursion frequency (REF) for that coordinate. This REF is Slater's "frequency of upzeroes."¹ In this paper, the critical coordinates are taken to be the bond lengths $S_i + r_i^{\text{eq}}$. There are two sources of difference between bond distances calculated from an actual internal motion trajectory and from the SVA via Eq. (14) and the inverse of Eq. (12). Both are manifestations of the same approximation, and they cannot be discussed separately with rigor. First, there is the vari-

ation of the normal-mode energies with time, which results in the divergence of the SVA trajectory from the correct one. Second, as mentioned above, the SVA expresses bond displacements as linear combinations of the components of atomic displacements. The SVA rests upon this linear approximation to the internuclear distances. Without it, one cannot make the potential- and kinetic-energy functions be simultaneously sums of square terms of normal-mode coordinates and their time derivatives, respectively. As a result, the transformation of the equations of motion into noncoupled, normal-mode equations cannot be made. Hence, the two effects mentioned are, in reality, inseparable. However, for comparison purposes, we consider these two sources of difference to be independent of one another. To achieve this separability we introduce the IVA model, which might stand for intermediate vibration approximation (or, in view of the above discussion, the *inconsistent vibration approximation*). The IVA retains the linear relation of the SVA between the normal-mode and displacement coordinates, namely,

$$D = M^{-1} L Q, \quad (17)$$

but it uses the correct (nonlinear) expression [Eq. (11)] to calculate the internuclear distances S_i from the D obtained from Eq. (17). In this way, we may initiate a rigorous and an IVA trajectory with equal normal-mode energies from the same initial molecular configuration. The IVA makes the normal-mode potential-energy defect vanish initially.

Bond distances from the rigorous trajectory and the corresponding SVA and IVA approximate trajectories are obtained as a function of time. A counting procedure determines the frequency with which a given bond distance achieves a critical length, i.e., the REF. In the limit of infinitesimal vibration amplitudes, the rigorous, SVA, and IVA REF's are, of course, all equal. The REF's described in Sec. VII. A. 5 are obtained from long-time (rather than phase) averages over the rigorous and approximate trajectories. The "long" times involved are no greater than 2×10^{-12} sec, a restriction dictated by the accuracy of the numerical integration used.

V. MOLECULAR ENERGIES

It is convenient to discuss molecular energies in terms of "normal-mode energies," "Eckart energies," and "bond energies." The normal-mode energies were defined and described in Sec. IV. B. The others are described below.

A. Eckart energies

The total kinetic energy of the molecule can be expressed^{33d} in terms of the coordinates and velocities of the nuclei with respect to the Eckart axes and the angular velocity ω of these axes with respect to the laboratory-fixed ones. This expression is

$$T = T_v + T_r + T_{vr}, \quad (18)$$

where T_v , T_r , and T_{vr} are the kinetic energies of vibration, rotation, and vibration-rotation interaction (i.e., Coriolis energy), respectively, given by

$$T_v = \frac{1}{2} \sum_{i=1}^3 m_i \dot{\mathbf{x}}_i \cdot \dot{\mathbf{x}}_i, \quad (19)$$

$$T_r = \frac{1}{2} \sum_{i=1}^3 m_i (\omega \times \mathbf{x}_i) \cdot (\omega \times \mathbf{x}_i), \quad (20)$$

and

$$T_{vr} = \omega \cdot \sum_{i=1}^3 m_i [(\mathbf{x}_i - \mathbf{x}_i^{eq}) \times \dot{\mathbf{x}}_i]. \quad (21)$$

In terms of the Euler angles ψ , θ , and ϕ , the vector ω has the Eckart system components

$$\begin{aligned} \omega_x &= \dot{\theta} \sin\psi - \dot{\phi} \sin\theta \cos\psi, \\ \omega_y &= \dot{\theta} \cos\psi + \dot{\phi} \sin\theta \sin\psi, \\ \omega_z &= \dot{\phi} \cos\theta + \dot{\psi}. \end{aligned} \quad (22)$$

The somewhat more complicated expressions for the Euler angular velocities in terms of atomic positions and velocities follow straightforwardly from differentiation of the expressions for the angles themselves given and implied in Sec. IV. A.

B. Bond energies

A weak-coupling treatment of unimolecular reactions, such as RRK theory, requires that the sum of oscillator energies be constant in time. If the oscillators are taken to be the normal modes, this amounts to assuming that $\sum_{i=1}^3 \epsilon_i$ is a good constant of the motion. However, the RRK oscillators are sometimes¹¹ associated with the bonds of the molecule. Although the dynamical concept of bond energy in polyatomic molecules is fraught with difficulties, we pursue it here to examine its possible utility in RRK or alternative interacting oscillator theories. We choose as an intuitive definition of the energy of bond i the expression

$$E_i = T_i + V_i, \quad (23)$$

where the bond potential energy is given in Eq. (2) and the bond kinetic energy T_i is given by

$$T_i = \frac{1}{2} \mu_i |(\dot{\mathbf{x}}_k - \dot{\mathbf{x}}_j) \cdot \rho_i|^2. \quad (24)$$

In Eq. (24), the indices i , j , and k are a cyclic permutation of 1, 2, 3, and ρ_i is a unit vector along the bond i from atom $A^{(j)}$ to $A^{(k)}$, and μ_i is the reduced mass of the $A^{(j)} A^{(k)}$ pair:

$$\mu_i = m_j m_k / (m_j + m_k). \quad (25)$$

Equation (24) is invariant under rotations of the coordinate system.

The terms V_i in Eq. (23) are the pairwise potentials of our models. At all times, their sum is the total potential energy of the molecule. On the other hand, the bond kinetic energies do not necessarily sum to the total vibrational kinetic energy, T_v . Indeed, a decomposition of the atomic velocities resulting from various normal-mode *kinetic* energies in A_3 shows that $\sum_{i=1}^3 T_i$ will differ initially from T_v by +50%, +41%, -40%, and +13% when the initial energy is entirely in the form of kinetic energy and the modes excited are symmetric stretch, bend, asymmetric stretch, and equal amounts of all three, respectively. These relative errors in $\sum_i T_i$ are independent of the total energy and do *not* vanish in the

limit of small vibration amplitudes. Thus, the sum of neither the bond energies nor the normal-mode energies will equal the total vibration energy in general. From an exact solution to the dynamic problem, one can determine whether $\sum_{i=1}^3 E_i$ or $\sum_{i=1}^3 \epsilon_i$ is the better constant of the motion.

VI. NUMERICAL METHODS

A. Trajectory initialization

In order to integrate the equations of motion (3) and (4), one needs initial values for the 12 components of the quantities X_1 , X_3 , P_1 , and P_3 corresponding to desired initial properties. Initially, the Eckart and fixed axes are taken, without loss of generality, to be coincident. The initial orientation of the equilibrium geometry (see Fig. 2) is fixed by taking \mathbf{r}_2^{eq} parallel to and in the same sense as the $\hat{\mathbf{x}}$ unit vector, again without loss of generality.

In all the calculations to be reported here, the initial normal-mode kinetic energy is zero; that is, all trajectories are begun at a turning point for all the oscillators. Thus, all vibrations are initially in phase; this requirement represents a considerable loss of generality for the initial conditions. With the exception of a very few special cases, however, the phase lock is quickly broken by oscillator interaction during the trajectories. Thus, the dynamics of in-phase initiated trajectories should not be qualitatively different from out-of-phase initiated ones.

The initial rotational energy and axis of rotation are input parameters. The magnitude of the initial angular velocity is obtained from the inverse of Eq. (20):

$$\omega = \left(\sum_{i=1}^3 m_i |\hat{\omega} \times \mathbf{x}_i|^2 / 2I_r \right)^{1/2}. \quad (26)$$

The initial atomic velocities are then determined through the relation

$$\dot{\mathbf{x}}_i(0) = \omega \times \mathbf{x}_i(0), \quad (27)$$

where the initial atomic positions are fixed by Eq. (17) and the choice of initial normal-mode (potential) energies.

B. Integration of equations of motion

The equations of motion are integrated by an Adams-Moulton 5th order predictor/6th order corrector routine.^{34,35} Adams-Moulton coefficients for these and other orders are given in Sec. II. 4.1.1. of Ref. 30. The table of past derivatives required by this routine is filled initially by a 4th order Runge-Kutta-Gill³⁶ operating at half the time step size. A typical step size is about 4.2×10^{-16} sec. Typical trajectories involve about 4000 such steps.

Energy and angular momentum are conserved to better than 0.001% during these trajectories. When an A_3 trajectory is initiated from normal-mode (potential) energies of $\epsilon_{\text{sym}} = \epsilon_{\text{asym}} = \epsilon_{\text{bend}} = 40$ kcal mol⁻¹ and integrated for 3.36×10^{-12} sec (molecule time) at a step size of 8.4×10^{-16} sec, momentum reversal at the termination and further integration leads to recovery of four deci-

mal digits of the initial coordinates and momenta.

VII. RESULTS AND DISCUSSION

A. Vibration dynamics

The Slater and RRR theories mentioned in the Introduction assume that rotation has a negligible effect on the rates of intramolecular energy transfer in unimolecular reactions. In Sec. VII. B, we investigate the validity of this assumption. Here we report results of our study of the dynamics of molecules undergoing vibrations only. These studies suffice to check the validity of the small-coupling and small-vibration approximations.

The initialization of all trajectories to be discussed in the present section is accomplished by giving the molecules varying amounts of normal-mode potential energy. The momenta conjugate to the normal coordinates are initially zero, and the vibrations begin in phase with each other.

1. Zero-point energy dynamics

The zero-point vibrations of H₂O exemplify the characteristics of all the C_{2v} molecules we studied (D₂S, H₂Se, NO₂, SO₂, and F₂O). The zero-point energy of our H₂O model calculated from the normal mode frequencies is 13.32 kcal mol⁻¹. When each normal mode of the molecule is given its zero-point potential energy, the total vibrational energy is found to be 14.65 kcal mol⁻¹. This discrepancy was discussed in Sec. IV. B.

The O-H bond distances are given as functions of time in Fig. 3(a) for vibrations in which each normal mode of the molecule is initially given its zero-point potential energy. These distances appear to a certain extent to exchange amplitude with one another. In this respect, their behavior is similar to that of tuned, coupled pendulums.³⁷ This analogy is reinforced in Fig. 3(b). Indeed, when one pendulum is started swinging while the other is at rest, the pendulums exchange their total energy, which is approximately the case for the OH bond energies. The pendulum analogy also suggests the mechanism for this exchange. When weakly coupled pendulums are swinging with energy in only one of the normal modes for that system, no energy transfer between the pendulums takes place. It is only when two normal modes are excited that the pendulum energy exchange occurs, and the exchange rate is related to the beat frequency (i.e., frequency difference) between the two modes.

In the water molecule, the normal modes which have the strongest effect on the valence bond lengths are the symmetric and asymmetric stretches. The pendulum analogy predicts that those bonds should exchange energy with a 7.5×10^{-14} sec period, which is associated with the symmetric-asymmetric beat frequency of 1.33×10^{13} sec⁻¹ for this model. This is precisely the observed bond energy exchange period. The phenomenon persists even under the perturbation of the bending motion, as long as the symmetric and asymmetric modes energies are good constants of the motion.

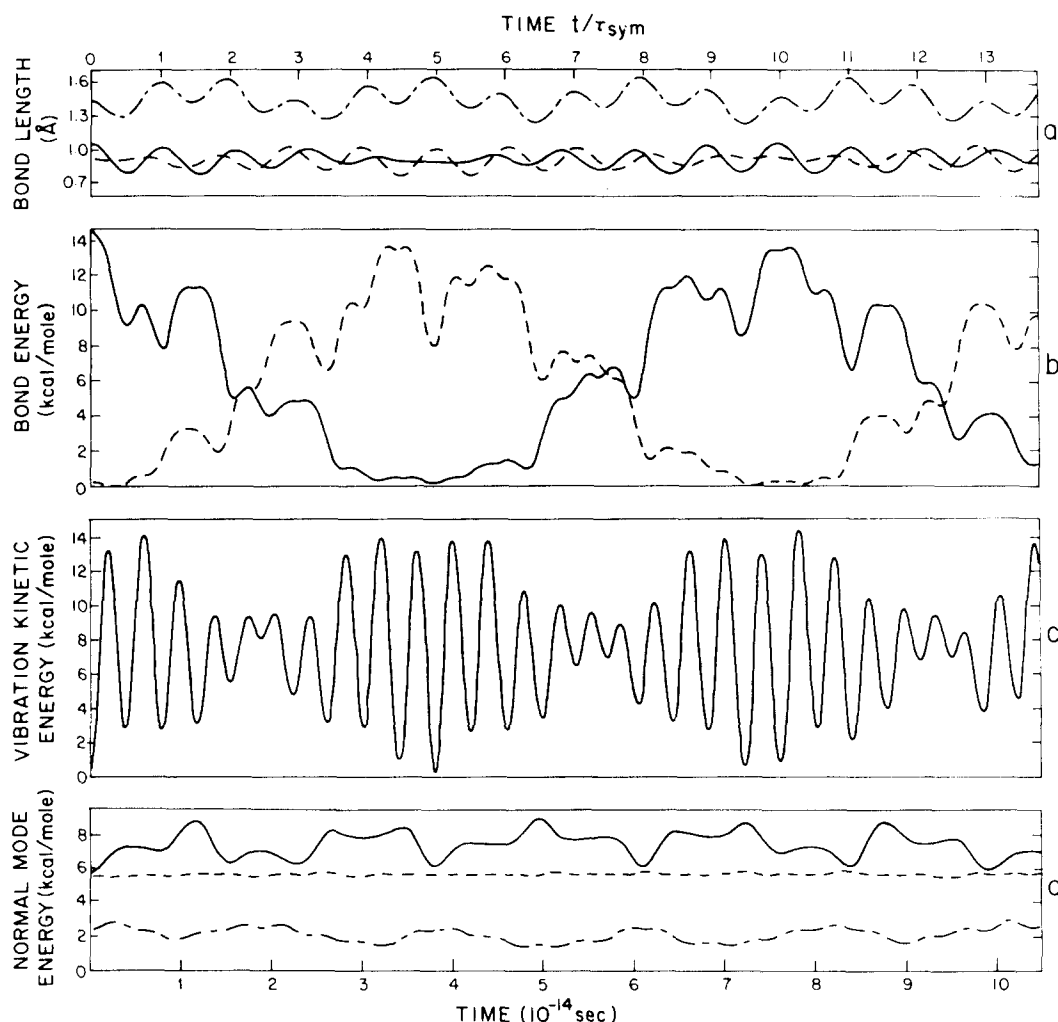


FIG. 3. Zero-point energy of H_2O . τ_{sym} is the symmetric-stretch vibration period of 7.62×10^{-15} sec for the model. (a) Bond lengths: —, OH; ---, OH; - - -, HH. (b) Bond energies. Same convention as in (a). HH omitted for clarity. (c) Kinetic energy of vibration. (d) Normal-mode energies: —, symmetric stretch; ---, asymmetric stretch; - - -, bend.

The vibrational kinetic energy of the molecule T_v shown in Fig. 3(c) demonstrates the beat rather clearly. When the energy of one of the O-H bonds is zero, T_v oscillates with twice the frequency of the excited bond. (The factor 2 comes from the existence of two turning points per bond oscillation.) As the other bond becomes excited, the O-H bonds oscillate $\pi/2$ out of phase with one another, such that the sum of the nuclear kinetic energies is approximately constant. Since the O-H bonds acquire equal energy twice in every beat cycle, the envelope of T_v has twice the beat frequency.

The nonconservation of normal-mode energies is clearly seen in Fig. 3(d), although for the zero-point vibrations the fluctuations in the normal-mode energies are small (less than about $\pm 10\%$) relative to the total energy. There appears to be no long-term exchange of energy among the modes. The ordering of normal-mode energies is conserved; that is, the symmetric stretch always has the most energy, and the bending vibration has the least. The short-term (10^{-14} sec) fluctuations are not large enough to obscure the bond energy beat.

The bond energy beat phenomenon is common to all

the C_{2v} triatomic molecules studied, but it is not a result of their symmetry. It follows instead from the proximity of the symmetric and asymmetric molecular frequencies in these molecules. The small frequency differences insure beat frequencies much lower than, and well separated from, the vibration fundamentals. On the other hand, the widely separated fundamental frequencies in ClN^{18}O give beats which are lost in the fundamentals themselves. For this reason, the bond energies in zero-point vibrating nitrosyl chloride in Fig. 4(b) do not show even roughly the exchange periodicity observed in Fig. 3(b) for water. The low frequency, high amplitude bend in nitrosyl chloride renders the SVA a more severe approximation for that molecule than it was for H_2O . The normal-mode energies of zero-point vibrating ClN^{18}O shown in Fig. 4(c) exhibit greater relative variation than those of H_2O given in Fig. 3(d). The very small amplitude vibrations (not shown) arising from an input of only 1/10 of the nitrosyl chloride zero-point energy into the molecule results in normal-mode energies which fluctuate by only a few percent during the trajectory.

For the set of molecules we studied, the normal-

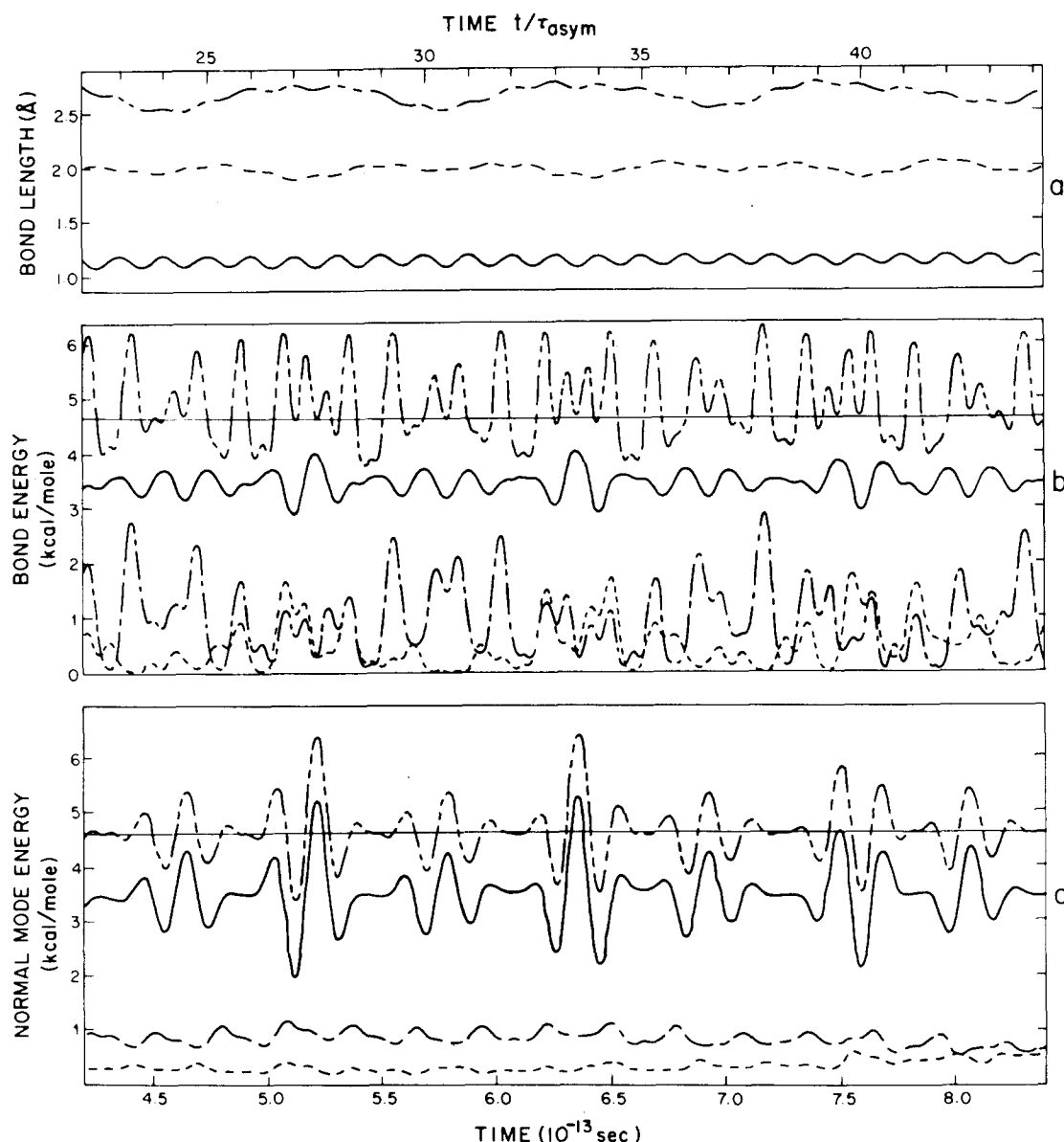


FIG. 4. Zero-point energy vibration of ClN^{18}O . τ_{asym} , the asymmetric-stretch period for the model, is 1.950×10^{-14} sec. (a) Bond lengths: —, N^{18}O ; ---, Cl^{18}O ; - · - ·, NCl . (b) Bond energies. Same convention as in (a). - · - ·, sum of bond energies. Horizontal line represents the constant total energy. (c) Normal mode energies: —, asymmetric stretch; ---, symmetric stretch; - · - ·, bend; - · - · - ·, sum of normal mode energies. Horizontal line represents the total energy.

mode zero point energies are in the range of 0.5–6.3 kcal/mole, and none of the normal-mode energies vary during a trajectory by more than ± 1.5 kcal mol^{-1} . These results thus define the degree to which the SVA furnishes an adequate description of zero-point vibrations. Although the classical deviations from SVA are small in absolute magnitude for ground vibrational states, they should manifest themselves in the quantum-mechanical treatment as well,¹⁸ and therefore they can be expected to play a role in the interpretation of vibrational spectra.

The inconstancy of these normal-mode energies does not imply failures of either classical mechanics or the numerical integration procedure. Neither does it suggest that molecules do not have stationary vibrational-rotational states. The classification of these states in terms of sets of good quantum numbers can no longer

be made in terms of the usual normal mode quantum numbers. A generalization of this concept invoking curvilinear coordinates may, however, be possible.³⁸

2. Highly energized A_3

To investigate the dynamics of molecules at energies approaching those necessary for reaction, the relatively rigid, symmetric A_3 and the loose, asymmetric ClN^{18}O molecules are given half their respective dissociation energies in four ways. First, all this energy is put into one normal mode at a time, and the dynamics of an initially pure normal-mode vibration is determined. Then the same amount of energy is partitioned equally among the three normal modes. This latter procedure will be called "mixed mode" initiation hereafter.

The "dissociation" of A_3 requires the rupture of two

O₂-like bonds with the expenditure of at least 119.43 kcal mol⁻¹ for each bond.¹⁹ In what follows, half the dissociation energy of A₃ will be denoted by $D_0 (= 119.43 \text{ kcal mol}^{-1})$.

From the D_{3h} symmetry of A₃, it is clear that any energy input to the molecule as pure symmetric stretch causes it to execute that normal-mode motion forever. The rigorous conservation of pure D_{3h} motion is of value in checking the accuracy of integration routines but does not elucidate normal-mode coupling phenomena. Not only the symmetry of the motion but also the symmetric normal-mode energy is conserved.

When A₃'s bend mode is excited instead, the subsequent dynamics do *not* conserve the corresponding normal-mode energy which varies periodically with the bend frequency.³⁰ At an initial excitation of D_0 , the amplitude of this variation is about 20 kcal mol⁻¹ or about 15% of the total energy. The bend mode is a motion having C_{2v} symmetry which *is* conserved even though the bend normal-mode energy varies. About 3% of the total energy appears in the symmetric stretch mode which periodically exchanges this small amount of energy with the bend mode. The remainder of the variation in bend normal-mode energy appears directly as variation in total normal-mode energy because there is *no* exchange of energy between the bend and asymmetric stretch modes. Initially pure bend motion does not excite asymmetric stretch motion even though those two modes are degenerate in A₃. They are uncoupled by the high symmetry of the motion.

In contrast, when the energy D_0 is put into asymmetric stretch, the resultant molecular vibrations are not even approximately confined to that mode (see Fig. 5). The rocking of the Eckart axes under asymmetrically stretching A₃ (see Sec. IV) produces small Coriolis forces. Since such forces³⁹ on nucleus i are directed along the vector $\dot{x}_i \times \omega$, they convert asymmetric stretch into the bending motion, and vice versa. The asymmetric-stretch normal-mode energy cannot go to zero by this mechanism because the C_{2v} bend motion does not rock the Eckart axes. As the bending normal-mode energy rises to $0.7 D_0$, the weakened Coriolis forces begins to convert it back into asymmetric-stretch energy. Since half of this energy is exchanged in about 7.5×10^{-13} sec, we infer (although our integration did not extend far enough to verify this) that the complete exchange period is about 1.5×10^{-12} sec. This period is about 2 orders of magnitude smaller than those associated with collisions⁴⁰ between gas molecules at standard temperature and pressure (STP). Thus, one may assume that normal-mode energies are constant between collisions for A₃ molecules which are stretching asymmetrically with half their dissociation energy *only* if the product $FT^{1/2}$ of the pressure times the square root of the temperature is about 400 *times greater than at STP*. Such experimental conditions are very difficult to obtain!

The energy exchange normal modes between the degenerate bend and asymmetric stretch evident in Fig. 5(c) appears to be periodic. Its frequency is about 22 cm⁻¹. Let us assume that there exist two truly nonin-

teracting vibration modes (not the usual normal modes) which are periodic and have frequencies ω_1 and ω_2 . Since these noninteracting modes and the normal modes are not coincident, it follows that excitation of a single normal mode must excite a mixture of noninteracting modes. Hence, the pendulum analogy leads us to anticipate a normal-mode exchange frequency which is equal to the beat frequency of the noninteracting modes, i.e., $\omega_1 - \omega_2 = 22 \text{ cm}^{-1}$. This beat frequency goes to zero with decreasing vibration amplitude because the normal and noninteracting modes coincide at vanishing displacements, and the noninteracting modes thus acquire the degeneracy of the normal bend and asymmetric-stretch modes. Clearly, those noninteracting modes are no longer degenerate at a vibration energy of D_0 . Note that the vibration frequencies in Fig. 5(a) are the same for all the bonds indicating that they are being "driven" by a single cyclic coordinate. However, they are not oscillating with the 1370 cm⁻¹ expected for ω_{asym} (see Table I). Inspection of the bond 3 curve in Fig. 5(a) reveals that it is initially in phase (fully compressed) with the τ_{asym} tic marks at the top of the figure. However, by the time 30 (normal-model) asymmetric periods have passed, bond 3 (and both the other bonds) is -180° out of phase with τ_{asym} marks. Hence the frequency of the bonds and *a fortiori* that of the noninteracting (asymmetric-stretch-like) vibration mode, $\omega_1 \sim (29.5/30) \times \omega_{\text{asym}} = 1347 \text{ cm}^{-1} \sim \omega_{\text{asym}} - 22 \text{ cm}^{-1}$! By this and the beat frequency formula, the other noninteracting (bend-like) mode has a frequency $\omega_2 \sim \omega_{\text{asym}} = \omega_{\text{bend}}$. This result might have been anticipated from the fact that bending vibrations do not produce Coriolis forces since they do not rock the Eckart axes. Note that the frequency of the noninteracting mode ω_1 depends on the total energy E . This is anharmonic behavior from a rigorously harmonic model.

In neither pure bend nor (initially) pure asymmetric-stretch vibration is there any appreciable excitation of the high frequency symmetric stretch. The symmetric normal-mode energy is at all times very close to zero as indicated by the lowest of the curves in Fig. 5(c) (which stays at all times very close to the abscissa axis).

When each of the normal modes in A₃ are excited an energy equal to $D_0/3$, the bend and asymmetric-stretch modes (not shown) are again weakly coupled and exchange energy with a period of 1.6×10^{-12} sec. The detailed nuclear motions, as well as the overall exchange, are very nearly periodic. This may be further evidence of the nonergodicity of harmonic phase space suggested by the results of Bunker^{24a,b} and of Nordholm and Rice.¹⁷

It can be seen [Figs. 5(b) and 5(c)] that the RRK oscillator energies do not sum to the total vibrational energy if the oscillators are associated with either the bonds or the normal modes of the molecule. Thus, the high-energy vibrations of the A₃ molecule rigorously satisfy neither Slater's assumption of constant normal-mode energies nor the RRK assumption that the oscillators are so weakly coupled that their energies sum with small error to the total vibrational energy of the molecule. It is unlikely that these conclusions depend upon the high symmetry of the A₃ molecule. In view of the artificiality of A₃ and the apparent malice in the choice

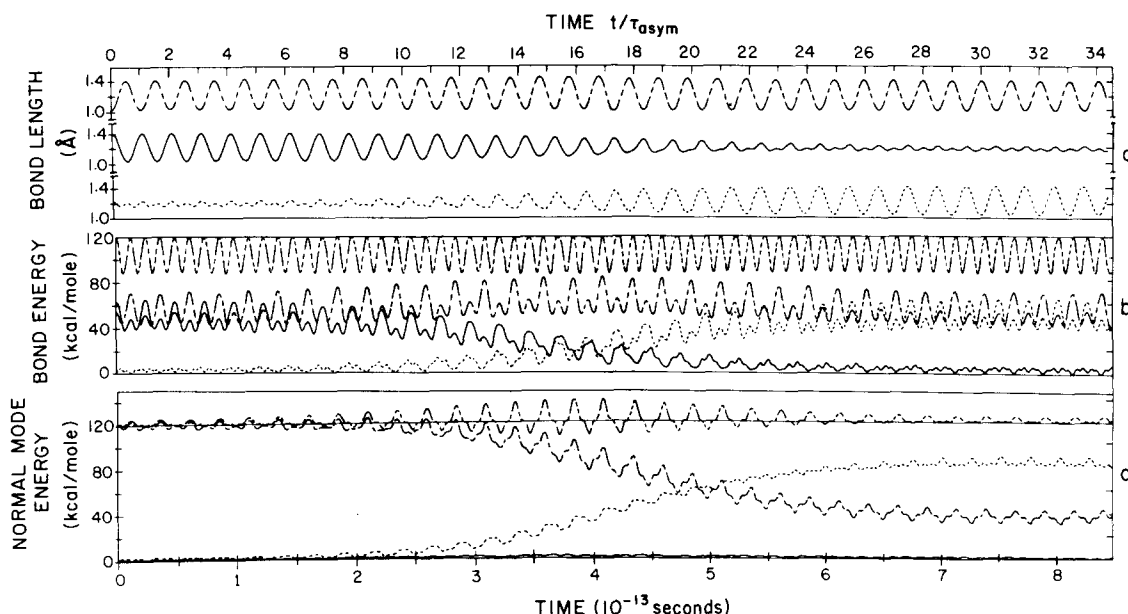


FIG. 5. High-energy asymmetric stretch in A_3 . Initial asymmetric stretch normal-mode potential energy equals $D_0 \sim 120$ kcal mol $^{-1}$. (a) Bond lengths: —, bond 1; $\circ\circ\circ$, bond 2; ---, bond 3. (b) Bond energies: —, bond 1; $\circ\circ\circ$, bond 2; ---, bond 3; and ---, sum of bond energies. (c) Normal mode energies: —, symmetric stretch; $\circ\circ\circ$, asymmetric stretch; ---, bend; ---, sum of normal mode energies. Horizontal line represents the constant total energy.

of degenerate vibrations, the study of a more realistic harmonic model is warranted; results of such a study are reported in the next section.

It should be noted that the detailed nuclear motions in this study are, no doubt, quite sensitive to the initial phases δ_i of the normal-mode vibration. With the exception noted in Sec. VII. A. 5, all the trajectories in this study used $\delta_i = 0$ for all i in Eq. (14). This means that the molecule is initially in its most distorted geometry. With $\delta_i = \pm\pi/2$ (equilibrium geometries), the observed normal-mode energy scrambling might not have been as severe (though separate calculations indicate that it does not vanish). The corresponding trajectories might allow the molecule to seek out distorted geometries more closely approximating those of the true independent vibrations associated with the excited normal modes. This possibility was not investigated. However, if any set of normal-mode initial phases yield trajectories with grossly inconstant normal-mode energies, as long as this set is not highly nonrepresentative of typical trajectories, the utility of the small-vibration approximation for the description of detailed molecular dynamics is called into question.

3. Highly energized $CIN^{18}O$

The dissociation energy⁴¹ of the N-Cl bond in nitrosyl chloride is 38.4 kcal mol $^{-1}$. For comparison with the results of the preceding section, we introduce only half this energy, or 19.2 kcal/mole, into the normal modes of the molecule.

The vibrational mode of highest frequency is essentially the vibration of the N=O bond [Fig. 2(a)]. Solution of the equations of motion shows that 19.2 kcal mol $^{-1}$ of energy in this normal mode is conserved to within 0.7%

for the 8.4×10^{-13} sec over which we integrated the trajectory. Symmetric stretching of nitrosyl chloride [diagrammed in Fig. 2(c)] is not a stable mode of motion (Fig. 6) for energies as high as 19.2 kcal mol $^{-1}$. During the first 5×10^{-13} sec of the trajectory, the symmetric-stretch normal-mode energy is reasonably constant. However, a steady increase in bending normal-mode energy gives rise to bend amplitudes large enough for the molecule to pass through linearity at 7.25×10^{-13} sec [Fig. 6(a)]. As a result of this gross distortion from equilibrium geometry, the normal-mode energies fluctuate rather chaotically from about 7 to 10×10^{-13} sec after initialization [Fig. 6(c)]. The normal-mode energy defect in this mode is insignificant compared to the 150% and 100% defects observed in the bend amplitudes in those trajectories result in erratic variation of all the normal-mode and bond energies. The sum of the oscillator energies fluctuates by more than half the total energy of the molecule in the case of mixed-mode initialization (see Fig. 7).

Thus, for energies large enough to be of interest for unimolecular reactions the normal-mode energies in our harmonic model for $CIN^{18}O$ are not conserved over periods of time sufficiently long to be used as constants of the motion between collisions in the gas phase. Furthermore, coupling between RRR oscillators (either normal modes or bonds) is so strong that the sum of their energies can differ from the total energy by as much as a factor of 2. This implies that as much as half the energy of the molecule is tied up in oscillator interaction terms. Alternately, a wide range of total oscillator energies contribute to the dynamics of a molecule at a fixed internal energy. This behavior renders meaningless the use of such oscillators in either dynamical or statistical theories of unimolecular reactions, for the total energy becomes uncertain to an intolerable

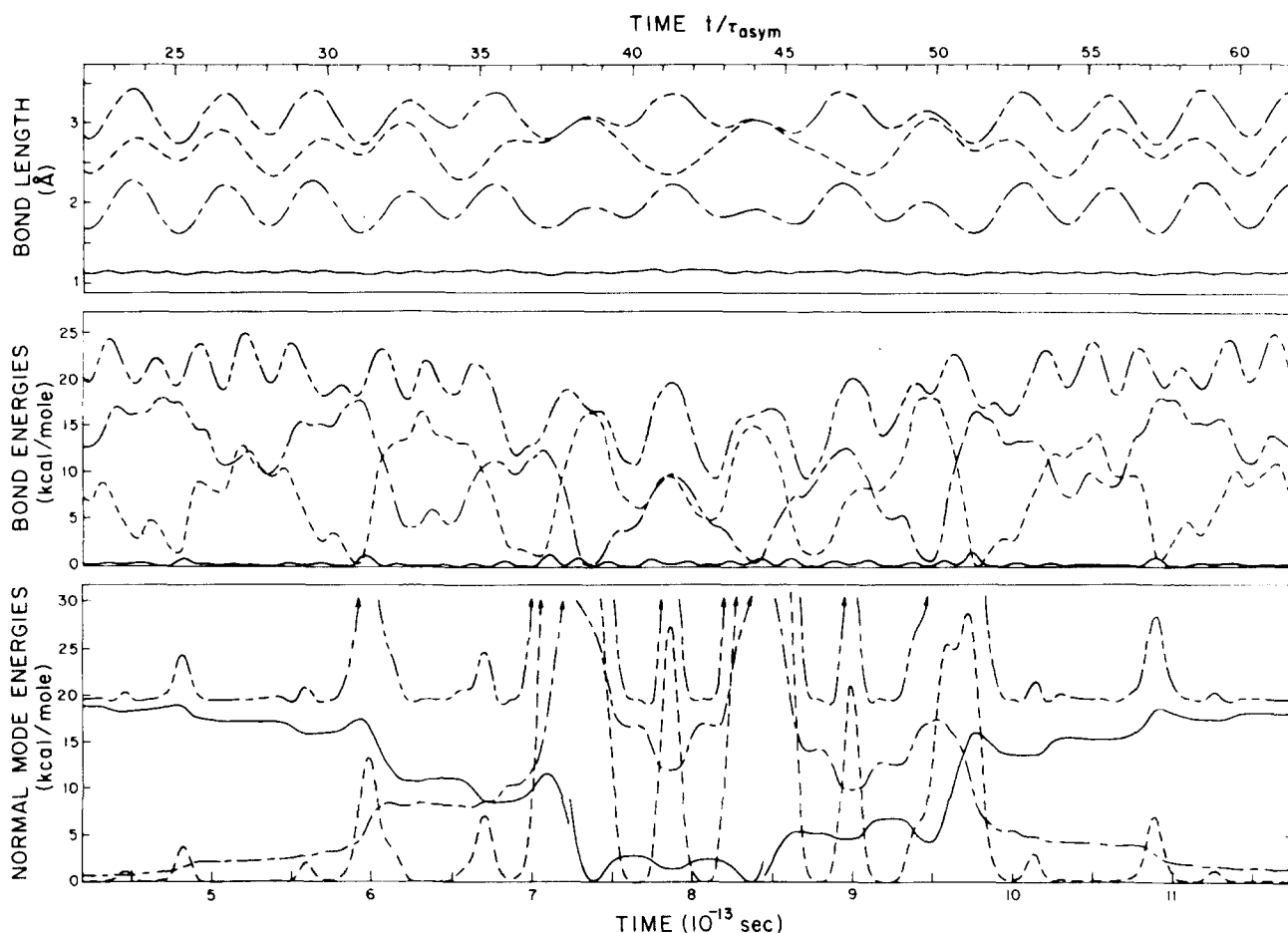


FIG. 6. High-energy symmetric stretch in ClN^{18}O . Initial symmetric stretch potential energy = 19.2 kcal/mol. (a) Bond lengths: —, N^{18}O ; ---, Cl^{18}O ; - · - ·, NCl ; - - - -, sum of the two smallest bonds, used as a linearity check. (b) Bond energies: —, N^{18}O ; ---, Cl^{18}O ; - · - ·, NCl ; and - - - -, sum of bond energies. (c) Normal-mode energies: —, asymmetric stretch; ---, symmetric stretch; - · - ·, bend; - - - -, sum of normal mode energies.

degree even at energies well below reaction thresholds. It suggests that densities of states (required in phase-space theories like RRKM) predicated upon the independent oscillator assumption may be in error even for rigorously harmonic potentials. The error, of course, must become arbitrarily small as the density of states becomes arbitrarily large. However, for light atom critical coordinates, associated with relatively low state densities, the effect may be significant.

While the SVA description of normal-mode vibration is fairly accurate at zero-point energies, it fails for dissociative energies. It is of interest to determine more precisely in what energy range the SVA may be considered valid.

4. Intramolecular energy exchange in ClN^{18}O

One may expect that the amount of mixing of one mode into another depends exponentially upon the time, since small perturbations produce small admixtures of modes of different symmetries, which, in turn, cause larger perturbations in an ever-accelerating growth. As we have seen in the preceding section, when 19.2 kcal/mol is put into the symmetric stretching mode of ClN^{18}O , the bending mode becomes excited. When the logarithm of the rising bend energy is plotted against time, as in

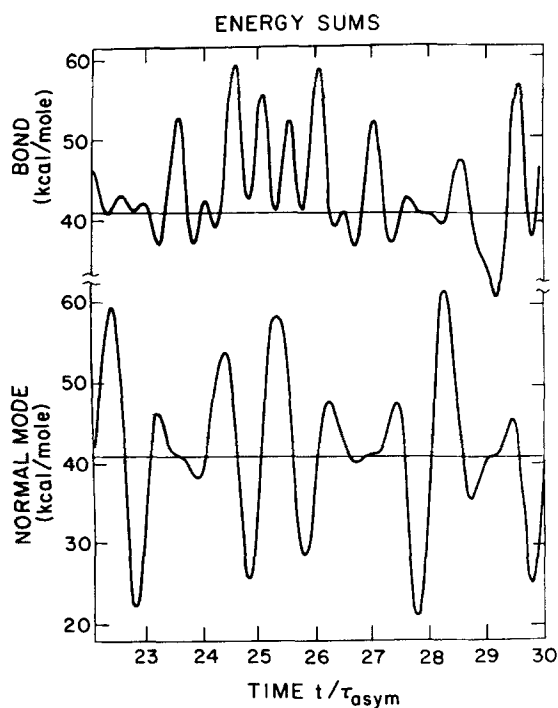


FIG. 7. Bond and normal-mode energy sums in ClN^{16}O . Initial energy input of 6.4 kcal mol⁻¹ into each normal mode. The horizontal lines represent the total energy.

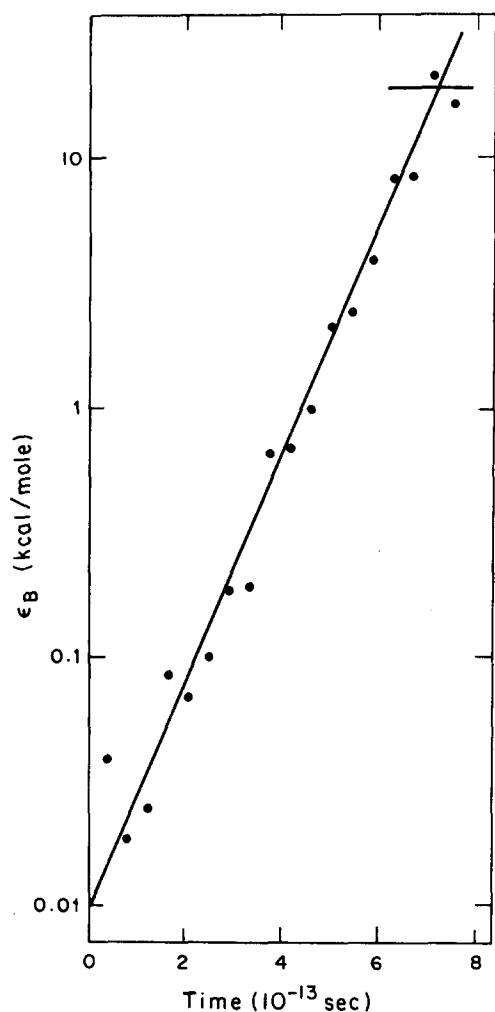


FIG. 8. Bending normal-mode energy as a function of time, by transfer from pure symmetric stretch in ClN^{18}O . Initial symmetric-stretch potential energy is 19.2 kcal/mol. Horizontal bar marks the total energy. Straight line indicates exponential growth of bend energy. Points lie on the trajectory-determined curve.

Fig. 8, the fit to a straight line (exponential growth) is seen to be good. This line may be taken to represent an average exponential growth. The time it takes the bending-mode energy to rise to the total energy of the molecule is a measure of the coupling between the two modes. We take the inverse of this time to represent a coupling frequency related to the period of growth and decay of bend energy observed in Fig. 6(c).

We plot a few much symmetric-bend coupling "frequencies" against total energy in Fig. 9. It is apparent from this figure that the SVA, which predicts that these coupling frequencies are zero, fails at energies greater than about 10 kcal/mol in nitrosyl chloride. Thus the attempt to utilize the SVA in a description of the dynamics of this harmonic molecule must be abandoned when the vibrational energy of the molecule is greater than approximately one-fourth the dissociation energy. At slightly greater energies, the intramolecular energy exchange rate is faster than the collision rate in gases even at moderately high temperatures and pressures.

5. Critical coordinate dissociation frequencies

The Slater harmonic unimolecular theory¹ requires an expression for the frequency of excursions of some critical coordinate past some critical configuration in order to predict dissociation or isomerization rate constants. Slater's formula comes from an analysis of the reactive excursion frequencies of a sum of sinusoidally varying normal modes of constant energy. Since the equations of motion of nonlinear harmonic molecules do not conserve the normal-mode energies, the reactive excursion frequencies calculated by Slater should not be expected to agree with those taken directly from trajectory calculations. In this section, we deal with the reaction excursion frequencies (REF) of interatomic bonds in A_3 and ClN^{18}O .

Figure 10 shows the bond distances as functions of time for both accurate and IVA (see Sec. IV.C) trajectories for mixed mode excitation of A_3 . The SVA bond distances (not shown) are within about 2% of the IVA values over the course of the trajectory. The nuclear motions in the IVA trajectories differ clearly from those in the accurate trajectory after about 3×10^{-13} sec. Nevertheless, the SVA and IVA REF's for bond 1 (Fig. 11) are seen to be very good approximations to the "rigorous" REF's, especially at large critical distances. It is conceivable that this might be an accidental result stemming from the high symmetry and concomitant degeneracy of the molecular frequencies in A_3 .

Since two of the vibration frequencies in A_3 are equal, none of these REF's is comparable with Slater's phase-averaged excursion frequencies.⁴² The REF's for in-phase mixed-mode initiation are found to be very different from those for 120° out-of-phase mixed-mode initiation. This is not true in the case of nitrosyl chloride, where it is found that the REF's are independent of the phase relation of the normal modes. It is significant in this regard that the molecular frequencies in nitrosyl

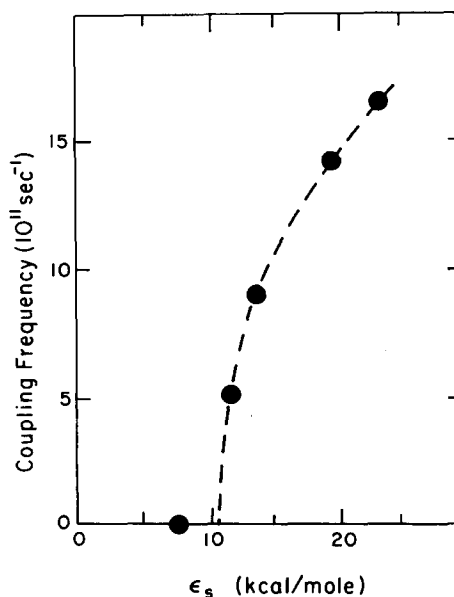


FIG. 9. Coupling frequencies for bending normal mode as a function of initial symmetric stretch energy in ClN^{18}O .

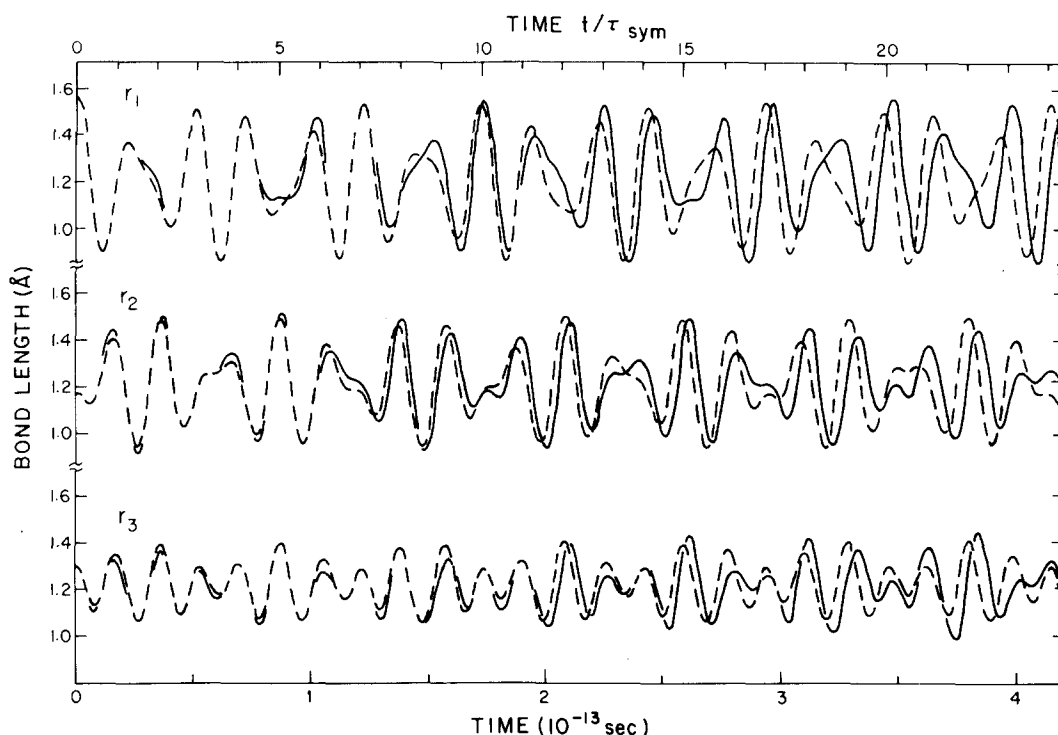


FIG. 10. The three bond lengths in A_3 as a function of time. All initial normal-mode potential energies are equal to $D_0/3$: —, accurate trajectories; ---, corresponding IVA trajectories.

chloride are highly noncommensurate (in a physical sense).

In the case of mixed-mode excitation, the IVA trajectory for nitrosyl chloride (Fig. 12) diverges more rapidly from the rigorous one than it does for A_3 . This relatively poor IVA (and SVA) representation is not reflected in the REF's. Figure 13 shows the REF's for N-Cl, the bond most easily broken in a dissociation reaction. Once again, for large critical displacements, the SVA and IVA give remarkably good descriptions of the actual REF's. The agreement implies that, although the trajectories of nitrosyl chloride are not themselves reproduced well by either approximation, the molecular quantities of greatest significance to the reaction rate, namely, the reactive excursion frequencies, are predicted fairly accurately by both the SVA and IVA. These conclusions apply to our harmonic CFF models vibrating with only half their "dissociation" energy. There is little reason to suspect that "dissociative" energy dynamics will alter these conclusions qualitatively.

Since the small vibration approximation fails, the coefficients α_{ri} , which relate the normal coordinates to the critical coordinate,²⁶ are in error. Thus, if $\alpha_{rj} = 0$ for some normal coordinate j , its contribution to the Slater reaction rate vanishes. However, we have shown that energy flows quite freely between the normal modes on a collision frequency time scale. Hence, energy initially deposited in normal coordinate j is indeed available to the reaction coordinate eventually. Thus the normal mode j should influence the reaction dynamics. What is required to correct this feature of Slater's theory is either (a) use of the (as yet unknown) true independent vibration modes and their associated α_{ri} , or (b) a description of "leaky" normal modes with some-

thing like an intramolecular master equation. Direct inclusion of intramolecular energy transfer has appeared in many theories.^{24b,43}

B. Vibration-rotation dynamics

The Slater and RRK theories of unimolecular reaction rates ignore the effect of rotation. Furthermore, the RRKM theory⁶ includes statistically the effects of rota-

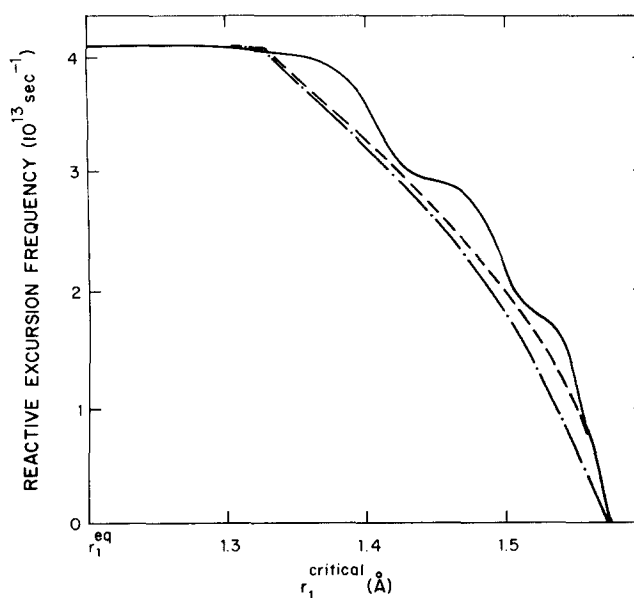


FIG. 11. Reactive excursion frequencies vs assumed critical length for bond 1 in A_3 . All initial normal-mode potential energies equal $D_0/3$: —, rigorous trajectory; ---, IVA; - · - · - SVA.

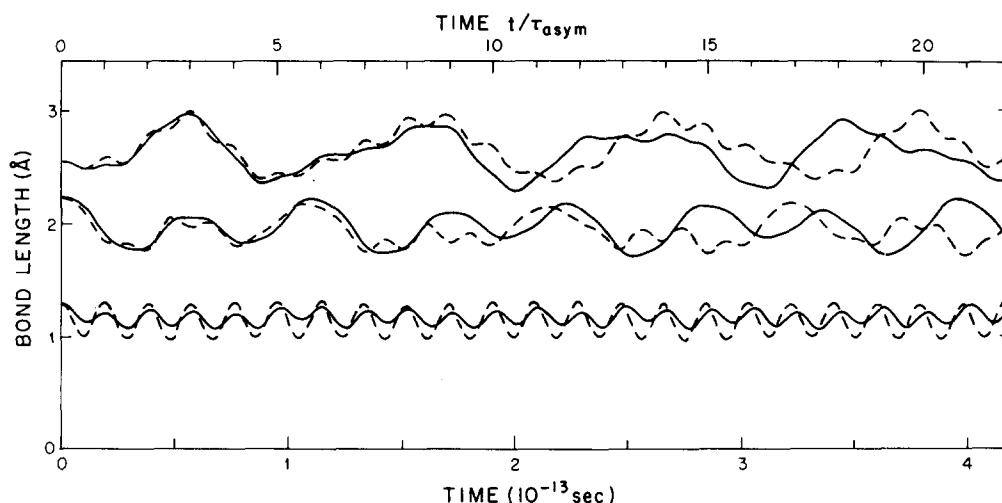


FIG. 12. Bond lengths in ClN^{18}O as a function of time. All initial normal-mode potential energies equal 6.4 kcal/mol: ---, rigorous trajectory; —, IVA.

tion in such a manner as to neglect vibration-rotation interaction effects on the density of states. The assumption implicit in all these theories is that rotation does not materially enhance intramolecular energy transfer. In Slater's theory, nothing excites intramolecular energy transfer, while in RRK theory, oscillator energy is already flowing at oscillation frequencies, and the molecular energy scrambling is thus saturated from vibration dynamics alone. In Sec. VII. A, we showed that intramolecular energy exchange is neither zero nor saturated under the influence of high energy vibration dynamics. Hence the assumption of the ignorability of rotation may be warranted in neither theory. In this section, we test this assumption for rotational energies comparable to (a) those found in gases at moderate temperatures and (b) dissociation energies.

1. Low energy rotations

By the method outlined in Sec. VI. A, a rotational energy of $0.02 D_0 = 2.39 \text{ kcal mol}^{-1}$ is superimposed on the vibrationally excited molecules of Sec. VII. A. 2 and VII. A. 3. This rotational energy corresponds to $3/2 kT$, where $T = 800^\circ \text{K}$. At this temperature, gas phase reaction rates are appreciable. For the symmetric top rigid rotor A_3 , this energy⁴⁴ is close to the level with quantum numbers $K = J = 33$. The rotations to be discussed in this section are all in plane; that is, the axis of rotation is perpendicular to the molecular plane.

The bending mode in nonrotating A_3 is stable; that is, although the bend energy is not conserved, the vibrational C_{2v} symmetry is. No asymmetric stretch is excited from pure bend motion. However, the modest $0.02 D_0$ in-plane rotation causes these modes to mix strongly. All the vibration energy (about D_0) is exchanged between bend and asymmetric stretch with a period of only $4.4 \times 10^{-13} \text{ sec}$. The bend symmetry is broken by the rotational Coriolis forces, as discussed in Sec. VII. A. 2. These forces augment those already present in the asymmetric stretch, and when this mode has D_0 initial energy, the $1.5 \times 10^{-12} \text{ sec}$ pure vibration coupling period is reduced to $3.7 \times 10^{-13} \text{ sec}$ for a rotating molecule. Thus, these moderate molecular rotations more than quadruple the intramolecular energy

transfer rate in this case. This is not a minor perturbation.

When A_3 with mixed-mode excitation is given $0.02 D_0$ in-plane rotation, the $1.6 \times 10^{-12} \text{ sec}$ coupling period observed in the absence of rotation is reduced to $3.2 \times 10^{-13} \text{ sec}$. Here the intramolecular energy transfer rate increases by a factor of 5.

The high-energy vibrations of ClN^{18}O (Sec. VII. A. 3) exhibit, in the main, intramolecular energy transfer rates which are of the order of the molecular frequencies. It is clear that rotation cannot increase these rates by so dramatic a factor in a molecule that is nearly "scrambling saturated." Initially pure 19.2 kcal/mol symmetric stretch energy [Fig. 5(d)] remains approximately constant for about $6 \times 10^{-13} \text{ sec}$. As seen in Fig. 14(d), the addition of 2.39 kcal/mol of in-plane rotation reduces this metastable lifetime to about 3.7

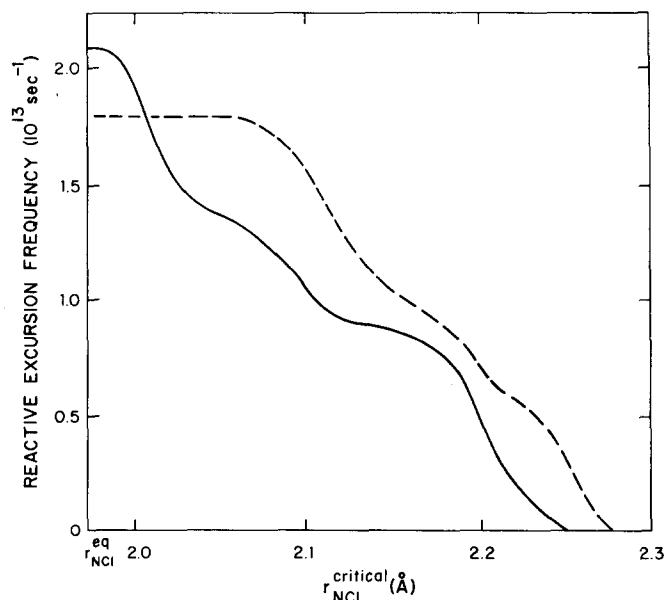


FIG. 13. Reactive excursion frequencies vs assumed critical length for the N-Cl bond in ClN^{18}O . All initial normal-mode potential energies equal 6.4 kcal/mol: —, actual trajectory; ---, IVA and SVA.

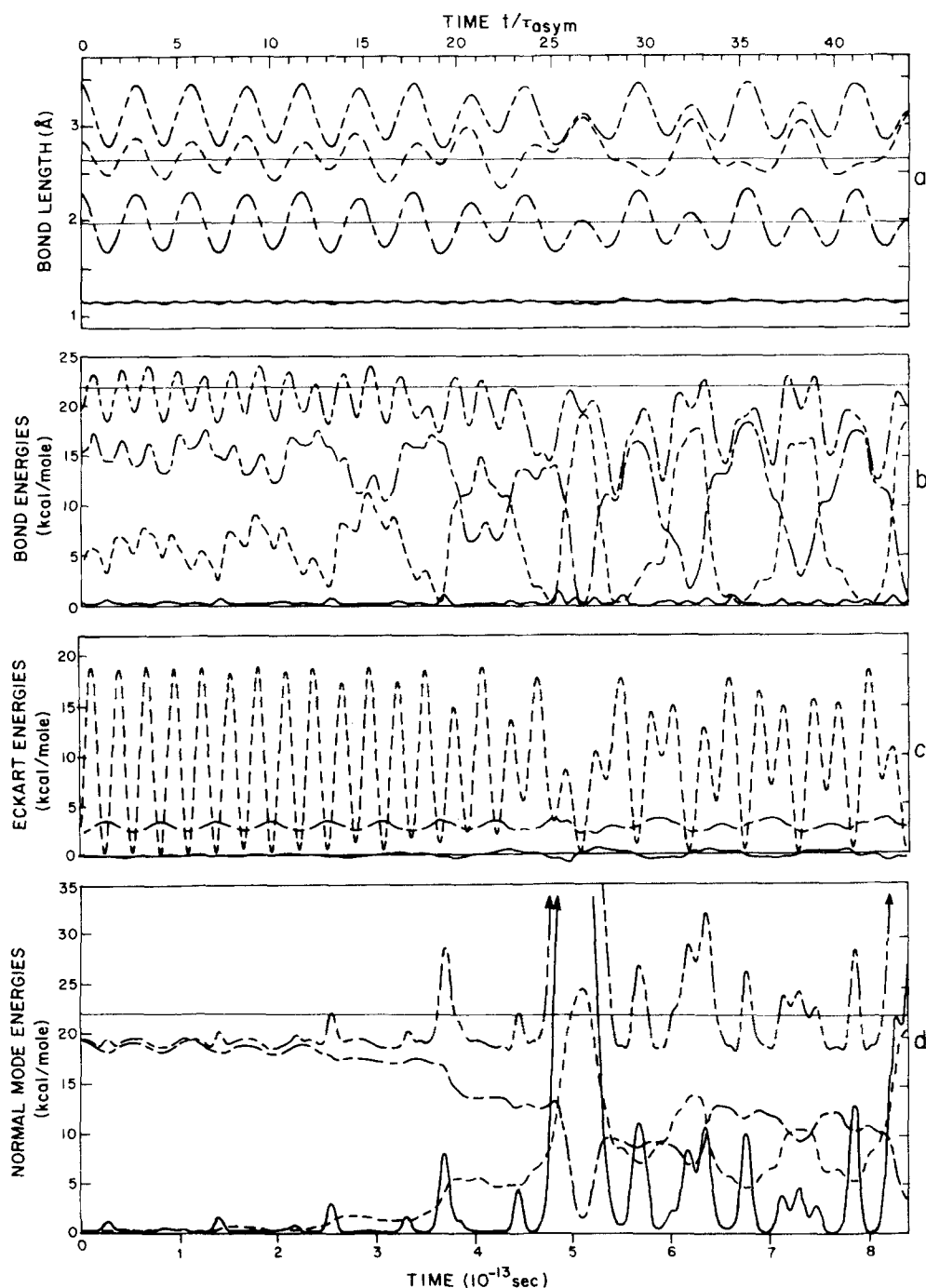


FIG. 14. Vibrating, rotating ClN^{18}O . Initial symmetric-stretch normal-mode potential energy equals 19.2 kcal/mol. Initial in-plane rotational energy equals 2.39 kcal/mol. See also Fig. 6. (a) Bond lengths: —, N^{18}O ; ---, Cl^{18}O ; - · -, NCl ; — · — · —, sum of two smallest bond lengths, which becomes tangent to the ClO curve for linear geometries. Horizontal lines represent equilibrium bond lengths appropriate to the curves which oscillate about them. (b) Bond energies: —, N^{18}O ; ---, Cl^{18}O ; - · -, NCl , and — · — · —, sum of bond energies. Horizontal line represents the total energy. (c) Eckart energies: — · — · —, vibration kinetic; — · —, rotation, —, Coriolis or vibration-rotation interaction. (d) Normal-mode energies: —, asymmetric stretch; ---, symmetric stretch; — · —, bend; — · — · —, sum of normal mode energies. Horizontal line represents the total energy.

$\times 10^{-13}$ sec. The rotation has enhanced the growth of the bending mode by a factor of 1.6—nonnegligible, but hardly as striking as in the A_3 case. The rotation alters the character of the vibrations after the rise of the bend energy. In the nonrotating case, this energy decays as if the molecule is going to exchange bend and symmetric-stretch energy periodically. Figure 14 shows that rotation has erased this periodicity. If the near periodicity of motion for the nonrotating case is a manifestation of the nonergodicity of harmonic phase space, it appears as if rotation destroys this property. This appears to contradict Bunker's observation^{24b} that rotation does not release the sufficiently energized but non-dissociating trajectories from their phase-space confines; however, Bunker's rotational energies were

probably smaller than those reported here.

With regard to the neglect of rotational dynamic effects in the contemporary unimolecular reaction rate theories, the following may be stated with some certainty for harmonic molecules. In relatively rigid complexes (i.e., dissociating species whose geometry is not much different from what it is at low energies), rotational effects are expected to be large, because vibration alone is insufficient to saturate the energy scrambling rates. On the other hand, rotation is likely to alter more seriously the details of the nuclear trajectories than the rate of intramolecular energy transfer in loose complexes, where vibrations alone suffice to scramble molecular energies freely.

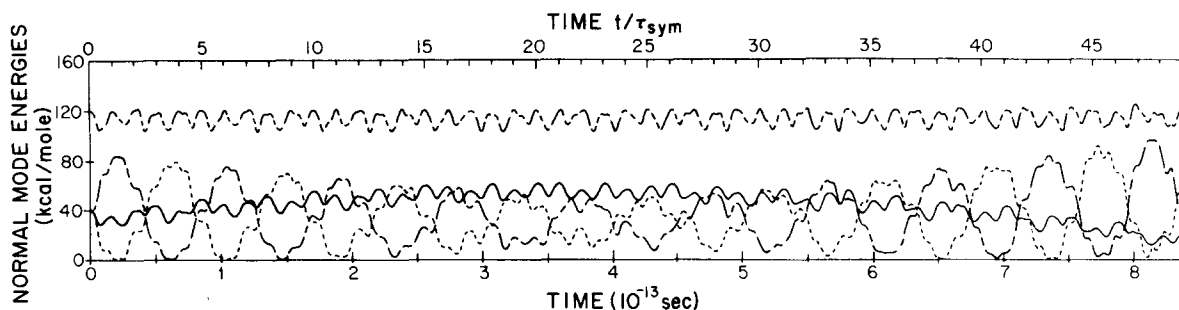


FIG. 15. Normal modes in high-energy vibrating, rotating A_3 . All initial normal mode energies equal 39.8 kcal/mol. Initial in-plane rotational energy equals 38.2 kcal/mol: —, symmetric stretch; ---, bend; - · -, asymmetric stretch; · · · ·, sum of normal-mode energies.

2. High energy rotations in A_3

For calculations reported in this section, the rotational energy is taken to be 38.2 kcal/mol, or about $\frac{1}{3} D_0$. This corresponds to a rotational temperature of about 13000 °K. Clearly, we are sampling molecules in the far tail of ordinary thermal rotational energy distributions. We use them not to suggest that they are representative but to examine the effects of very rapid rotation on vibrating systems. For a symmetric-top, rigid-rotor A_3 , this energy corresponds closely to that of the $K=J=135$ quantum level.

High energy tumbling (i.e., out-of-plane rotation about the x or y axes) causes the asymmetric stretch in A_3 to couple with the bend mode with a period of 4.2×10^{-13} sec. The inefficiency of tumbling with respect to enhancement of energy scrambling is now apparent, since the low-energy ($2.4 \text{ kcal mol}^{-1}$) in-plane rotation couples these modes with the shorter period of only 3.7×10^{-13} sec. As anticipated, then, high-energy in-plane rotation couples these vibration modes very strongly. The energy exchange period drops to 4.3×10^{-14} sec. Since the natural periods of both bend and asymmetric stretch are 2.44×10^{-14} sec, this massive in-plane rotational excitation seems to have almost saturated the normal-mode coupling rate in this still molecular model.

Being separated from them in frequency, the symmetric stretch in A_3 does not couple well with the other normal modes. It couples to all the rotations, however, since symmetric stretch produces large changes in all three moments of inertia. Nevertheless, no combination of vibrations and/or rotations discussed thus far succeeds in exciting any appreciable energy in the symmetric mode. It is somewhat surprising, then, to find that with high-energy rotation about either the x or z axes, A_3 with initial mixed-mode excitation exhibits evidence of coupling of its symmetric stretch to the other modes. This is most clear in the case of in-plane rotation (Fig. 15), wherein the strongly coupled bend and asymmetric stretch modes exchange energies rapidly (0.8×10^{-13} sec) within an energy envelope which appears to be coupled to the symmetric-stretch energy. The latter fluctuates slowly (about 1.2×10^{-12} sec) over a range of about $\frac{1}{2} D_0$.

Thus, we conclude that rotational energies on the order of dissociation energies are capable of producing

intramolecular energy scrambling on time scales comparable to the molecular vibration periods even in very stiff harmonic models.

VIII. SUMMARY

We have shown that the Slater small-vibration approach to the classical dynamics of bent triatomic molecules is inapplicable at energies approaching those necessary for dissociation. Slater's assumption of constancy of the normal-mode energies fails for the harmonic ClN^{18}O model at energies above 25% of the molecule's dissociation energy. Despite this, Slater's formulas for reaction frequencies are shown to give values in good agreement with the actual reaction frequencies in our harmonic models.

The assumption of weak coupling between molecular harmonic oscillators, used in RRK theory, is shown to be a poor one at all energies, if the oscillators are taken to be the interatomic bonds. If, instead, the RRK oscillators are assumed to be the normal modes, they are indeed weakly coupled at energies of the order of zero-point levels. As the vibrational energy in the molecule approaches that necessary for reaction, however, the oscillators couple strongly, and not only their individual energies but also the sum of those energies fail to be constants of the motion by up to 100%. The difference between this sum and the constant total energy is the oscillator coupling energy (in the absence of rotation), which is not negligible, as assumed in RRK theory.

Great care must be exercised in applying either the RRK or Slater theories to interpret the results of infrared laser augmented decompositions.¹⁵

None of the theories mentioned treats the often significant dynamic effects of rotation on the intramolecular energy transfer rates. At rotational energies corresponding to 800 °K, the energy scrambling rates in ClN^{18}O vibrating with half its dissociation energy, are increased by 60%. The enhancement is larger in molecules more rigid than nitrosyl chloride. Nonergodicity effects observed in ClN^{18}O and triangularly-symmetric, relatively-rigid A_3 are easily destroyed by relatively small amounts of rotation, which must be included in unimolecular reaction rate theories which invoke such nonergodicity.

Thus, some basic assumptions about the dynamics

of molecules undergoing unimolecular reaction are shown to be inadequate when applied to the high-energy vibrations and rotations of the simple harmonic model for the bent triatomic molecule. We hope that the results reported here will serve as a useful guide for the construction of more realistic dynamical models for use in unimolecular reaction-rate theory.

*Supported in part by the Energy Research and Development Administration Report Code No. CALT-767P4-49. This work was begun while the authors were associated with the Department of Chemistry, University of Illinois, Urbana IL.

†Work performed in partial fulfillment of the requirements for the Ph.D. in Chemistry at the California Institute of Technology. Present address: The University of Texas at Dallas, Box 688, Richardson TX 75080.

‡Contribution No. 5290.

¹N. B. Slater, *Theory of Unimolecular Reactions* (Cornell U.P., Ithaca, NY, 1959), Chaps. 2, 5, 7, and 9.

²L. S. Kassel, *Kinetics of Homogeneous Reactions* (Chemical Catalog Company, New York, 1932), Chap. V and references therein.

³S. W. Benson, *Foundations of Chemical Kinetics* (McGraw-Hill, New York, 1960), Chaps. X and XI.

⁴H. S. Johnston, *Gas Phase Reaction Rate Theory* (Ronald, New York, 1966), Chap. 15.

⁵D. L. Bunker, *Theory of Elementary Gas Reaction Rates*, International Encyclopedia of Physical Chemistry and Chemical Physics, Topic 19 (Pergamon, New York, 1966), Chap. 3.

⁶For reviews of RRKM theory, see (a) P. J. Robinson and K. A. Holbrook, *Unimolecular Reactions* (Wiley, New York, 1972), and (b) W. Forst, *Theory of Unimolecular Reactions* (Academic, New York, 1973).

⁷L. Pauling and E. B. Wilson, Jr., *Introduction to Quantum Mechanics* (McGraw-Hill, New York, 1935), Sec. X-37, pp. 282-290.

⁸(a) G. Herzberg, *Molecular Spectra and Molecular Structure: II. Infrared and Raman Spectra of Polyatomic Molecules* (Van Nostrand, New York, 1945), pp. 159-191; (b) H. C. Urey and C. A. Bradley, *Phys. Rev.* **38**, 1969 (1931); (c) T. Shimanouchi, *J. Chem. Phys.* **17**, 245, 734, 848 (1949).

⁹Reference 1, Chap. 5.

¹⁰(a) E. Thiele and D. J. Wilson, *J. Phys. Chem.* **64**, 473 (1960); (b) N. B. Slater, *J. Phys. Chem.* **64**, 476 (1960).

¹¹Reference 2, Chap. V, Footnote 11.

¹²M. H. Hui and S. A. Rice, *J. Chem. Phys.* **61**, 833 (1974).

¹³K. Shobataki, Y. T. Lee, and S. A. Rice, *J. Chem. Phys.* **59**, 1435, 6104 (1973) and references therein.

¹⁴S. E. Buttrill, *J. Chem. Phys.* **61**, 619 (1974) and references therein.

¹⁵E. R. Lory, S. H. Bauer, and T. Manuccia, *J. Phys. Chem.* **79**, 545 (1975).

¹⁶Reference 1, p. 30, footnote.

¹⁷S. Nordholm and S. A. Rice, *J. Chem. Phys.* **61**, 203, 768 (1974); **62**, 157 (1975).

¹⁸L. I. Schiff, *Quantum Mechanics* (McGraw-Hill, New York, 1968), pp. 175-176. A dynamical variable is a classical constant of the motion if it has no explicit time dependence and its Poisson bracket with the Hamiltonian is zero. It is a quantum-mechanical constant of the motion if its associated operator commutes with the Hamiltonian, and again, there is no explicit time dependence. The relation between the commutator and the Poisson bracket given in Equation (23.9) of Schiff, namely, $[A, B] = i\hbar \{A, B\}$, verifies the statement made in the text, which refers only to dynamical variables which are defined both classically and quantum mechanically.

¹⁹G. Herzberg, *Molecular Spectra and Molecular Structure. I. Spectra of Diatomic Molecules* (Van Nostrand, Princeton,

NJ, 1950), 2nd ed., pp. 558-560.

²⁰J. R. Durig and R. C. Lord, *Spectrochim. Acta* **19**, 421 (1963).

²¹W. B. Eberhardt and T. G. Burke, *J. Chem. Phys.* **20**, 529 (1953).

²²(a) G. V. Calder and W. F. Giauque, *J. Phys. Chem.* **69**, 2443 (1965); (b) W. H. Evans, T. R. Munson, and D. D. Wagman, *J. Res. Natl. Bur. Stand.* **55**, 147 (1955). Calder and Giauque misquote Evans *et al.* by interchanging the ΔH_0° values for the dissociation of Cl_2 and I_2 .

²³E. Thiele and D. J. Wilson, *J. Chem. Phys.* **35**, 1256 (1961).

²⁴(a) D. L. Bunker, *J. Chem. Phys.* **37**, 393 (1962); (b) D. L. Bunker *ibid.* **40**, 1946 (1964); (c) D. L. Bunker, *ibid.* **57**, 332 (1972); (d) H. H. Harris and D. L. Bunker, *Chem. Phys. Lett.* **11**, 433 (1971); (e) D. L. Bunker and W. L. Hase, *J. Chem. Phys.* **59**, 4621 (1973).

²⁵For our purposes, phase space is metrically decomposable if trajectories can be trapped in some subvolume in the constant energy hypershell and are incapable of crossing the boundaries of that volume. In the SVA, all trajectories are so contained, since they may not wander into regions of the hypershell wherein the normal mode energies differ from their initial values.

²⁶Reference 1, pp. 58, 91. Slater's high-pressure rate constant is given by $k_\infty = \bar{\nu} \exp(-E_0/kT)$, where E_0 is the minimum energy for dissociation, k and T are the Boltzmann constant and absolute temperature, and the frequency factor $\bar{\nu}$ is taken to be the weighted root mean square of the normal-mode frequencies ν_i , namely,

$$\bar{\nu} = \left(\frac{\sum_{i=1}^n \alpha_{ri}^2 \nu_i^2}{\sum_{i=1}^n \alpha_{ri}^2} \right)^{1/2},$$

where the α_{ri} are defined by the expression which relates the normal-mode coordinates Q_i , to the reaction coordinate q_r :

$$q_r = \sum_{i=1}^n \alpha_{ri} Q_i.$$

²⁷N. C. Hung and D. J. Wilson, *J. Chem. Phys.* **38**, 828 (1963).

²⁸N. C. Hung, *J. Chem. Phys.* **57**, 5202 (1972).

²⁹The notation used in these equations will be defined by the following example. Let

$$P_i = P_{X_i} \hat{X} + P_{Y_i} \hat{Y} + P_{Z_i} \hat{Z}$$

and

$$\dot{X}_i = \dot{X}_i \hat{X} + \dot{Y}_i \hat{Y} + \dot{Z}_i \hat{Z}.$$

The equation $\dot{X}_i = \partial \mathcal{H} / \partial P_i$ will be taken to mean $\dot{X}_i = \partial \mathcal{H} / \partial P_{X_i}$, $\dot{Y}_i = \partial \mathcal{H} / \partial P_{Y_i}$, and $\dot{Z}_i = \partial \mathcal{H} / \partial P_{Z_i}$.

³⁰C. Parr, Ph.D. thesis, California Institute of Technology, 1969.

³¹See, for example, F. Villars, *Nucl. Phys.* **3**, 240 (1957).

³²C. Eckart, *Phys. Rev.* **47**, 552 (1935).

³³E. B. Wilson, J. C. Decius, and P. C. Cross, *Molecular Vibrations* (McGraw-Hill, New York, 1955): (a) Appendix I, p. 285; (b) p. 275, Footnote 1; (c) Chap. 4; (d) Chap. 11.

³⁴J. B. Scarborough, *Numerical Mathematical Analysis* (John Hopkins Press, Baltimore, MD, 1962), 5th ed., pp. 318-325.

³⁵This routine was extended from one donated to us by Dr. T. Latta.

³⁶S. Gill, *Proc. Cambridge Philos. Soc.* **47**, 96 (1951). This reference contains detailed treatment of the derivation and error analysis of the algorithm.

³⁷A. Sommerfeld, *Lectures on Theoretical Physics. Vol. I. Mechanics* (Academic, New York, 1964), pp. 106-110.

³⁸E. g., J. T. Houzen, P. R. Bunker, and J. W. C. Johns, *J. Mol. Spectrosc.* **34**, 136 (1970).

³⁹H. Goldstein, *Classical Mechanics* (Addison-Wesley, Reading, MA, 1950), pp. 135-140.

⁴⁰Reference 3, pp. 154-155, Table VII.2.

⁴¹The "classical" bond dissociation energy $D_e(\text{Cl}-\text{N}^{18}\text{O})$ is given by

$$D_e(\text{Cl}-\text{N}^{18}\text{O}) = \Delta H_0^\circ(\text{Cl}-\text{N}^{16}\text{O}) + \frac{hc}{2} \left\{ \sum_{i=1}^3 \omega_i(\text{ClN}^{16}\text{O}) - \omega(\text{N}^{16}\text{O}) \right\},$$

where the molecular frequencies are obtained from Refs. 15 and 14, and $\Delta H_0^\circ(\text{Cl}-\text{N}^{16}\text{O})$ comes from Refs. 17(a) and 17(b), which give $\Delta H_0^\circ(\text{ClN}^{16}\text{O} \rightarrow \text{N}^{16}\text{O} + \frac{1}{2}\text{Cl}_2)$ and $H_0^\circ(\frac{1}{2}\text{Cl}_2 \rightarrow \text{Cl})$, respec-

tively.

⁴²Reference 1, Chap. 4.

⁴³E.g., (a) J. W. Brauner and D. J. Wilson, *J. Phys. Chem.* **67**, 1134 (1963); (b) M. Solé, *Chem. Phys. Lett.* **1**, 160 (1967).

⁴⁴N. Davidson, *Statistical Mechanics* (McGraw-Hill, New York, 1962), p. 172, Eq. 11-7.